Biomass and Bioenergy, Volume 98, March 2017, pp. 182–193
DOI: 10.1016/j.biombioe.2017.01.020

Techno-economic analysis of biofuel production *via* bio-oil zeolite upgrading: an evaluation of two catalyst regeneration systems

Mobolaji Shemfe[a,b*], Sai Gu[c] and Beatriz Fidalgo[a]

[a]Bioenergy & Resource Management Centre, Cranfield University, Bedford, Bedfordshire, MK43 0AL, UK.
[b]Centre of Environmental Strategy, University of Surrey, Guildford, Surrey, GU2 7XH, UK
[c]Department of Chemical and Process Engineering, University of Surrey, Guildford, Surrey, GU2 7XH, UK.

ABSTRACT

Biofuels have been identified as a mid-term GHG emission abatement solution for decarbonising the transport sector. This study examines the techno-economic analysis of biofuel production *via* biomass fast pyrolysis and subsequent bio-oil upgrading *via* zeolite cracking. The main aim of this study is to compare the techno-economic feasibility of two conceptual catalyst regeneration configurations for the zeolite cracking process: (i) a two-stage regenerator operating sequentially in partial and complete combustion modes (P-2RG) and (ii) a single stage regenerator operating in complete combustion mode coupled with a catalyst cooler (P-1RGC). The designs were implemented in Aspen Plus® based on a hypothetical 72 t/day pine wood fast pyrolysis and zeolite cracking plant and compared in terms of energy efficiency and profitability. The energy efficiencies of P-2RG and P-1RGC were estimated at 54% and 52%, respectively with corresponding minimum fuel selling prices (MFSPs) of £7.48/GGE and £7.20/GGE. Sensitivity analysis revealed that the MFSPs of both designs are mainly sensitive to variations in fuel yield, operating cost and income tax. Furthermore, uncertainty analysis indicated that the likely range of the MFSPs of P-1RGC (£5.81/GGE – £11.63/GGE) at 95% probability was more economically favourable compared with P-2RG, along with a penalty of 2% reduction in energy efficiency. The results provide evidence to support the economic viability of the production of biofuels from upgrading of pyrolysis-derived bio-oil via zeolite cracking.

Keywords: zeolite cracking; bio-oil; Aspen Plus; fast pyrolysis; uncertainty analysis; techno-economic analysis

*Corresponding author: Centre for Environmental Strategy, University of Surrey, Guildford, Surrey, GU2 7HX, UK.' Email address: m.shemfe@surrey.ac.uk

1 INTRODUCTION

CO_2 emissions from fossil fuel combustion and industrial processes are the key sources of global anthropogenic greenhouse gas (GHG) emissions and has been correlated with the steep rise in global mean temperatures since the beginning of the industrial revolution [1]. Currently, the international consensus tend towards urgent implementation of emission regulations and policies to drive the deployment of sustainable alternatives to fossil fuels [2]. Moreover, the urgency for alternative fuel sources is driven by depleting fossil fuel resources and projected growths in global population and energy demand. In 2012, the transport sector accounted for 28% of global energy consumption, of which biofuels constituted 2.5% [3]. In order to meet the emissions target set for 2050, emission reduction of 16.1 Gt CO_2e has to be made in the transport sector. Biofuels are expected to supply 27% of global transport fuels by 2050, with the goal of reducing CO_2 emissions by 13%. In pursuance of biofuels as a viable GHG emission reduction pathway, more research is required in the areas of process development and energy efficiency [1,4].

Biomass can be converted into biofuels *via* three main conversion methods including chemical, biochemical and thermochemical processes. Biofuels derived from these conversion processes are classified into various generations based on the carbon source of the feedstocks. First generation biofuels are derived from sugars and lipids extracted from food crops *via* chemical and biochemical conversion methods. Second generation biofuels are derived from non-food sources, including lignocellulosic biomass, agricultural waste and dedicated energy crops *via* biochemical and thermochemical conversion processes. Third and fourth generation biofuels from microalgae and fast growing energy crops are becoming more prevalent in research with sustainability and carbon negativity as the main drivers. Most of the commercially available biofuels are of the first generation, comprising 3% of global transport fuel demand [5]. However, they have been linked with several issues, including spikes in the price of food crops due to competition for the same means of production, as well as limited GHG emission savings and conflicting land use issues [6–8].

Nevertheless, current efforts towards the commercialisation of biofuels focuses on second and third generation biofuels as they induce less strain on food supply and land use [6,7]. One of the thermochemical conversion routes for producing second generation biofuels that is attracting much interest is fast pyrolysis, as it produces a higher yield of bio-oil product (liquid fraction) than other thermochemical conversion pathways. Fast pyrolysis is the rapid thermal decomposition of biomass at temperatures between 450 and 600 °C in the absence of oxygen to produce non-condensable gases, bio-oil and char (solid residue). Bio-oil has been demonstrated as fuel for heat generation in boiler systems and power generation in some diesel engines [9,10]. Nevertheless, it is unusable in internal combustion engines due to its adverse properties, which are ascribable to its high oxygen content, low heating value and high acidity [11].

Bio-oil can be upgraded into advanced biofuels by traditional refinery processes specifically hydroprocessing and catalytic cracking. Hydroprocessing encompasses two main hydrocatalytic processes namely hydrodeoxygenation and hydrocracking. Operating conditions such as catalyst type, reactor temperature and pressure, and weight hour space velocity can influence the quantity and quality of biofuels derived from bio-oil hydroprocessing [12]. The major shortcomings of bio-oil hydroprocessing include high hydrogen consumption and severe pressure conditions required for operation [13–16]. An alternative bio-oil upgrading route is the catalytic cracking process. Catalytic cracking involves a series of reactions including dehydration, cracking, deoxygenation and polymerisation. The products from these reactions include gas, organic liquids, aromatic and aliphatic hydrocarbons, water and coke. An advantage of catalytic cracking over hydroprocessing is that it does not require hydrogen at high pressure. Nevertheless, it presents the drawback of rapid catalyst deactivation due to high coking rate [17].

Several catalysts have been employed for the catalytic cracking of bio-oil. Several experimental studies on the catalytic upgrading of bio-oil over zeolites (HZSM-5) reported a high concentration of aromatic hydrocarbons (about 83 wt.%) in the organic liquid product [18–21]. *In-situ* catalytic pyrolysis and *ex-situ* catalytic upgrading of pyrolysis vapours before condensation over HZSM-5 catalysts are gaining more ground [22–27]. The bio-oil product from catalytic pyrolysis is partially deoxygenated and contains a

higher concentration of aromatic hydrocarbons and phenols than the bio-oil product of non-catalytic pyrolysis [22]. Other catalysts different from zeolites, such as Al-MCM-41, Al-MSU-F and nano metal oxides have been applied to catalytic pyrolysis, also giving rise to partial reduction of the oxygenated compounds in bio-oil [28–31]. Nevertheless, results from these studies suggest that HZSM-5 catalysts are best suitable for upgrading biomass-derived oils as they improve the selectivity towards the hydrocarbons present in gasoline and diesel, and yield relatively more liquid than other catalysts [17,32,33].

An obstacle that could hinder the industrial deployment of bio-oil upgrading *via* zeolite cracking is the resultant high coke yields that accompanies the process [34]. The utilisation of conventional Fluid Catalytic Cracking (FCC) units (cracking reactor integrated with a single stage regenerator) has been proposed for the cracking of bio-oil [35]. Nevertheless, bio-oil generates more coke (up to 20 wt.%) [19] compared with typical feeds to FCC units (1–5 wt.%) [36]. Generally, the regenerator of FCC units operates at complete or partial (incomplete) combustion modes [36]. High coke yields from the cracking of bio-oil will inevitably result in very high coke-burn temperatures in the regenerator when operating in a complete combustion mode and cause rapid deactivation of catalysts. Furthermore, extreme coke-burn temperatures in the regenerator without a proper heat rejection mechanism can upset the thermal balance between the cracking reactor and the catalyst regenerator [34,36]. Catalyst regeneration at partial combustion mode, on the other hand, leads to moderate regeneration temperatures, however, the exiting gas from the regenerator has a high concentration of CO and requires additional burning to CO_2 to meet emission standards. Thus, there is a need for innovative process designs for zeolite cracking of bio-oil with appropriate regeneration systems. The regeneration systems considered in this study are based on designs in the refining industry specifically used for cracking of resid (high molecular weight) feeds that are prone to severe coking. As zeolite cracking of bio-oil is also prone to severe coking, the two main designs used for resid cracking in the refinery industry were evaluated in this study to ascertain their techno-economic potential for catalyst regeneration in the bio-oil zeolite cracking process.

Techno-economic analysis (TEA) is a valuable research tool for exploring the technical and economic feasibility of conceptual process designs. Several studies of the techno-economic analysis of fast pyrolysis of biomass and bio-oil upgrading *via* zeolite cracking have been published [37–39]. Nonetheless, to our knowledge, the TEA of bio-oil upgrading *via* zeolite cracking along with the evaluation of the regeneration system options is non-existent in literature. This study examines the techno-economic analysis of biomass fast pyrolysis and bio-oil upgrading *via* zeolite cracking with emphasis on the catalyst regeneration system. A process scheme with two regenerators operating in sequence (P-2RG) and a scheme with a single regenerator fitted with a cooler (P-1RGC) are compared regarding energy efficiency and profitability. A sensitivity analysis is carried out to evaluate the influence of economic parameters on the profitability of the designs. In addition, Monte Carlo simulations are conducted to assess uncertainties in the estimated parameters and their effect on profitability.

2 METHODS

Fig. 1 depicts the overall methodology employed in this study. It entails model development, equipment sizing and costing, profitability analysis via discounted cash flow method, sensitivity analysis and uncertainty analysis *via* Monte Carlo simulation.

2.1 Process overview

Fig. 2 depicts the overall process diagram. It consists of six main technical sections: (i) bio-oil production *via* fast pyrolysis (A100); (ii) zeolite cracking of bio-oil (A200); (iii) products separation (A300–A302); (iv) catalyst regeneration (A400); (v) steam cycle (A500); and, (vi) gas cleaning (A600). In A100, bio-oil is generated *via* the fast pyrolysis process. The liquid bio-oil product is then transferred to the zeolite cracking section. In A200, bio-oil is vapourised by hot zeolite catalysts and undergoes dehydration, cracking, deoxygenation and polymerisation reactions to form non-condensable gases, organic vapours and coke. The products from A200 are then fed into A300 to separate catalyst and coke from the mixture of hot vapours and gases. Zeolite catalyst is regenerated by combustion of the coke in

A400. The catalyst is reactivated, and heat for the upgrading reaction in A200 is simultaneously generated. Excess heat from the regeneration system is used to generate power in A500. In the liquid recovery section (A301), the liquid product is separated from non-condensable gases. The liquid product from A301 then goes into the product conditioning section (A302) to isolate the oil phase from the aqueous phase. Finally, the oil phase is fractionated into the final products consisting of light organics, aromatic hydrocarbons and heavy residue.

2.2 Model development

The model was implemented in Aspen Plus® V8.4. The following subsections elaborate the model development of the technical sections (A100–A600).

2.2.1 BIO-OIL PRODUCTION (A100)

Bio-oil production (A100) comprises of biomass pre-treatment, fast pyrolysis and electricity generation. More details of the model for this section can be found elsewhere [40]. In brief, the plant capacity is based on 72 t/day (wet basis) of pine wood assumed with a moisture content of 25 wt.% and particle size of 20 mm. The biomass is fed to grinding and drying operations to achieve the specifications of the pyrolysis reactor, i.e. 10 wt.% moisture content and 2 mm particle size. The pre-treated biomass is converted into non-condensable gases (NCG), organic vapours and char in the pyrolysis reactor. The pyrolysis reactor was modelled based on chemical reaction kinetics of the three biopolymer components of biomass: cellulose, hemicellulose and lignin [41]. The fast pyrolysis model was validated against experimental results reported by Wang *et al.*[42]. Char is separated from the mixture of gas and vapours by high-efficiency cyclones and subsequently fed into a combustor. The vapour product is directly quenched at 49 °C using previously stored bio-oil, and the NCG is separated and compressed to the combustor. Char and NCG are then combusted to provide process heat for the pyrolysis reactor and drying operation. The residual heat is utilised for steam generation, which is expanded to generate electric power of 0.24 MW.

The bio-oil is produced at a flow rate of 1,608 kg/h and supplied to the zeolite cracking section (A200) for upgrading. Table 1 shows the chemical composition of the bio-oil product from A100.

2.2.2 ZEOLITE CRACKING (A200)

The bio-oil feed is preheated to 283 °C by a fired heater prior to being injected into the fluidised bed reactor. The reactor is essentially a riser, where the bio-oil is vaporised by heat carried by hot catalyst. Reliable kinetic models of the reactions occurring in the zeolite cracking reactor are scanty in literature due to the complex physical and chemical properties of bio-oil. Thus, the zeolite cracking reactor was sequentially simulated by the Yield reactor and Fluid bed models provided in AspenPlus® to represent product distribution and bed hydrodynamics. In the yield reactor, the product distribution is specified at 370 °C and weight hourly space velocity (WHSV) of 3.6 hr^{-1} based on experimental data reported in [19,21] (see Table 2). These authors studied the catalytic upgrading of fast pyrolysis bio-oil over HZSM-5 in a fixed bed micro-reactor. They concluded that several factors including reactor temperature, zeolite to silica-alumina ratio and WHSV influence product distribution and hydrocarbon selectivity [21], and found that the maximum concentration of aromatic hydrocarbons in the zeolite crackate was 69 wt. % of the organic fraction at 370 °C, and WHSV of 3.6 hr^{-1}

The bio-oil is then fed along with hot HZSM-5 catalyst into the FluidBed model. Laumontite was selected as the model compound of the catalyst due to similar physical properties with HZSM-5. The superficial velocity of the fluidising gas was determined by Ergun equation assuming a bed voidage of 0.9. The catalyst diameter was specified at 65 μm and, consequently, it was classified as a Geldart A particle. The Fluid bed model assumes an ideal adiabatic mixing between the hot catalyst and bio-oil feed to determine the outlet stream temperature at 370 ℃ The fluidisation in the riser is aided by dry nitrogen gas fed at 100kg/h. The reaction products comprised of gas, upgraded vapours and coke. These products were sent to the product separation area (A300 to A302).

2.2.3 PRODUCT SEPARATION AREA (A300–A302)

In A300, the entrained catalyst fines are separated from the gas fraction (gas products and carrier gas) in two high-efficiency cyclones in parallel to achieve a separation efficiency of 0.99. The spent catalysts are fed into the regeneration section A400. The remaining stream of hot vapours and NCG are sent into a cooler, where the temperature of the mixture is quenched to 35 °C. The quenched stream is sent to a flash drum operating at 35 °C and 1 bar (A301). The thermodynamic relationship in the flash drum was modelled by the Non-random two-liquid activity coefficient model. In the flash drum, the inlet stream is separated into three phases: an NCG phase, an aqueous phase (predominantly H_2O), and an oil-rich organic phase. The oil phase is then fractionated into its constituent compounds in a distillation column modelled by the RradFac unit model (A302). Table 3 shows the final fuel products from A302. The light ends from the distillation column and the gas separated in the flash drum are sent to a knock-out drum in order to remove moisture in the mixture before going into a stack.

2.2.4 CATALYST REGENERATION (A400)

Two regeneration systems of the spent catalyst were considered in this study: (i) Two-stage regeneration (partial combustion and complete combustion) system, P-2RG; and, (ii) Single stage regeneration system fitted with a catalyst cooler, P-1RGC.

2.2.4.1 Two-stage regenerator (P-2RG)

Fig. 3 depicts the process flow diagram of bio-oil zeolite cracking incorporated with the two-stage regeneration system.

The two-stage regenerator (P-2RG) considers coke combustion in two phases: the first stage operates at partial combustion and the second stage operates at complete combustion. P-2RG was simulated by two successive Gibbs reactors, which calculates the multi-phase equilibrium by minimising Gibbs free energy. The thermodynamic relationship of the Gibbs reactors was modelled by the Peng-Robinson-Boston Mathias Equation of State. In the first regenerator, coke is combusted in an air-deficient environment. The temperature of the first stage regenerator is controlled at 700 ℃at a stoichiometric air-to-coke ratio of 0.53.

The catalyst is separated by a cyclone at 700 ℃and charged back to the reactor riser. The exiting gas from the first stage regenerator, which is high in CO composition is sent to the second stage regenerator to undergo complete combustion into CO_2 at 1609 ℃. The heat generated in the second stage regenerator is used to produce superheated steam for subsequent power generation in A500.

2.2.4.2 Single stage regeneration with a catalyst cooler (P-1RGC)

Fig. 4 shows the process flow diagram of zeolite cracking integrated with the single stage regenerator fitted with a catalyst cooler. The regenerator was simulated by a Gibb's Reactor. The complete combustion of coke in the regenerator occurred at 1611 ℃to produce CO_2, H_2O, and NO_x. The catalyst cooler was simulated by a counter-current heat exchanger. The cooler is assumed to be fitted in the dense region of the regenerator to regulate heat and maintain the regenerator temperature at 700 ℃. In addition, it was assumed that the dense bed is well-mixed with an even temperature distribution to allow efficient heat transfer between the catalyst bed and the water. The cold water side of the heat exchanger is supplied with water at a 50 bar pressure to generate superheated steam at 503 ℃. The superheated steam is subsequently utilised to drive a turbine for power generation in A500.

2.2.5 POWER GENERATION (A500)

The heat generated from P-2RG and P-1RGC is used to produce steam for electric power generation. For both designs, steam power cycle was simulated by a counter-current heat exchanger, feed water pump, condenser and steam turbine. The thermodynamic property of the water section of the heat exchanger was modelled by the NBS/NRC Steam table provided in Aspen Plus. Superheated steam is generated at 503 ℃ and supplied to the steam turbine, which is specified at 80% isentropic efficiency and 95% mechanical efficiency to produce electric power.

2.2.6 GAS CLEANING (A600)

For both regeneration schemes, the exiting gas from the regenerator is sent to a Venturi scrubber to remove particulate matter including catalyst particles and residual volatile gases. The Venturi scrubber was

selected due to its low capital cost compared with other gas cleaning technologies. The gas is fed into a single-throat venturi scrubber at a velocity of 17.05 m/s and temperature of 80 ℃ The Venturi scrubber and mist eliminator were simulated by a Vscrub model and Flash separator, respectively. In the Venturi scrubber, particulate matter entrained in the flue gas is trapped by free flowing water at a volumetric flow rate of 8.04 m^3/s. Pressure drop in the scrubber was calculated by Calvert's model. The entrained droplets produced by the scrubber is separated in a mist eliminator at 2 bar. Nothnagel equation of state was specified as the property method of the Venturi scrubber and mist eliminator.

2.3 Energy efficiency

The energy efficiencies of the two processes were calculated by dividing the total energy produced by the system by the total energy supplied to the system. Eq. 1 illustrates the formula for energy efficiency.

$$\eta_{plant} = \frac{\dot{m}_o \cdot LHV_o + W_o}{\Sigma_i(\dot{m}_i \cdot LHV_i) + \Sigma W_i + \dot{Q}_i} \quad (1)$$

Where $\dot{m}_o$ is the mass flow rate of bio-hydrocarbon products and LHV_o is the corresponding lower heating value. W_o is the electricity generated by the processes. Similarly, $\dot{m}_i$ and LHV_i represents the mass flow rate and lower heating value of biomass feed, respectively. W_i is total electricity required to operate process equipment including compressors, pumps, air blowers, and cyclones. Q_i represents the heat duty of hot utility.

2.4 Process economics

2.4.1 COST ESTIMATION

Equipment sizing and cost estimation were carried out in Aspen Process Economic Analyzer® V.8.4 (APEA).The unit operations developed in Aspen Plus were mapped to the appropriate equipment cost models in APEA in order to perform sizing calculations and estimate the equipment purchase costs. The costs employed in this study are based on Q1. 2013 cost data. An exception to this approach was made in sizing and cost estimation of the pyrolysis reactor, riser for zeolite cracking and regenerators—all fluidised

bed vessels. The cost of the pyrolysis reactor and regenerators were estimated from the scaling equation in Eq. 2 using values reported by Wright *et al*., 2010 as the basis for estimation.

$$C_1 = C_O \cdot \left(\frac{S_1}{S_O}\right)^{0.6} \quad (2)$$

Where C_1 is the estimated cost with the size of S_1 and C_o is the base cost with the size of S_o.

The cost of the zeolite riser was based on the specified geometry of the vessels within the hydrodynamics operational regime limit. Capital cost was estimated by Lang factorial method. The hypothetical location of the plant is North-Western England. Thus, the UK cost template provided in APEA was applied. The assumptions made in estimating the total operating costs are presented in Table 4.

2.4.2 PROFITABILITY ANALYSIS

The profitability of the designs were evaluated using the discounted cash flow (DCF) method. First, the net present value (NPV) was computed using Eq. 3.

$$NPV = -C_T + \sum_{n=1}^{N=t} \frac{\phi\dot{m}(1-T_n) - O_n}{(1+r)^n} \quad (3)$$

Where C_T is the initial captial investment, ϕ is the fuel price, $\dot{m}$ is the fuel yield of the plant, t is the plant life, O_n is the annual operating cost and T_n is income tax. For the DCF analysis, the plant was assumed to operate for a 20 year period (t) at a required rate of return (r) of 10%. In addition, an income tax of 40% was applied to the DCF calculations. Next, the minimum fuel selling price (MFSP) was determined by setting NPV tozero, whilst other variables in equation 3 were held constant. The economic assumptions adopted for DCF analysis are presented in Table 5.

2.5 Sensitivity analysis

Sensitivity analysis was used to measure the effect of variations in process and economic parameters on profitability. The effect of key parameters including fuel product yield, capital cost, operating cost, income tax and the discount rate on the MFSP were examined. The criterion for selecting these parameters was based on their direct relationship with profitability, in other words, they are directly linked to the

calculation of the MFSP. A ±30 % range was adopted for the sensitivity analysis. Although the specified range for the sensitivity analysis allows uncertainties in parameter estimates to be individually evaluated, it does so deterministically without considering the inherent unpredictability of the studied parameters.

2.6 Uncertainty analysis *via* Monte Carlo method

Stochastic variations were introduced to the parameters *via* Monte Carlo simulations. Triangular probability distribution was assumed for all the parameters due to the lack of adequate statistical data [44]. The same approach was adopted in recent uncertainty studies of biomass conversion processes for parameters that lack sufficient data [38,45]. Table 6 shows the range of variation of the expected values of the parameters.

3 IN ORDER TO GENERATE RANDOM SAMPLES, A USER-DEFINED FUNCTION (UDF) WAS DEVELOPED IN PYTHON™. THE UDF WAS DYNAMICALLY LINKED TO AN ECONOMIC CALCULATION WORKSHEET IN MICROSOFT EXCEL® IN ORDER TO REDUCE COMPUTATIONAL TIME. THE SIMULATION GENERATED 10,000 SAMPLES, AND THE CORRESPONDING MFSPS WERE RETURNED. RESULTS AND DISCUSSION

3.1 Process performance

Table 7 illustrates the mass and energy balances obtained from Aspen Plus simulation of the two process schemes.

The process model estimated that a 3,000 kg/h fast pyrolysis plant processed 1,608 kg/h bio-oil. The pyrolysis process by-products (char and NCG) were combusted to provide heat, which drives the pyrolysis reactions and steam generation in an integrated miniature steam cycle. Therefore, the bio-oil production section (A100) is energy sufficient and does not require utility heating [40]. Moreover, section A100 produced net electricity of 240 kWh. Before entry into the cracking reactor (A200), the bio-oil is preheated by a hot utility with heat duty of 0.55 MW. The pre-heated bio-oil is upgraded *via* zeolite cracking to produce 448 kg/h of fuel. It should be noted that there is no distinction between the fuel yields from the two process schemes since both processes only differ in regenerator designs (A400). Nevertheless, the two

models differ in electric power consumption, the amount of heat generated from coke combustion and the electricity generated. The P-2RG design generated 896 kWh of electricity while P-1RGC generated 747 kWh of electricity. In addition, P-2RG consumed less power compared to that required by P-1RGC. The difference in electric power consumption was attributed to the load required to drive the air blower of P-1RGC.

The energy efficiencies of P-2RG and P-1RGC were 54% and 52%, respectively. The 2% difference in the energy efficiencies can be attributed to the fact that both designs generated slightly different electricity with the same product yields. The economic implications associated with the minimal difference in the observed energy efficiencies are evaluated in Section 3.2.

3.2 Economic analysis

Fig. 5 shows the capital and operating costs of P-2RG and P-1RGC. The total capital costs of P-2RG and P-1RGC were estimated at £13.2 MM and £12.1 MM, respectively.

The higher capital cost observed in P-2RG compared with 1-PRC was attributed to the additional equipment cost of the secondary regenerator required in P-2RG. The total operating costs of P-2RG and P-1RGC were estimated at £5.0 MM and £4.7 MM, respectively. Allocation of the constituent operating costs of the two designs is illustrated in Fig.6. It can be seen in Fig. 6 that the higher operating cost observed in P-2RG compared with P-1RGC, are attributable to higher maintenance and 'other' costs, which includes capital charges and insurance cost.

The MFSPs of P-2RG and P-1RGC were estimated at £7.48/GGE and £7.20/GGE, respectively. The relative difference in the capital and operating costs of P-2RG in reference to P-1RGC, estimated at 9.09 % and 6.38 %, respectively, resulted in a higher minimum fuel selling price in the case of P-2RG. The slightly better energy efficiency shown by P-2RG does not seem to be sufficient to justify the extra cost associated with the incorporation of a secondary regenerator and the resultant higher MFSP. The combined economic and energy efficiency analysis points toward the single regenerator fitted with a cooler P-1RGC as the preferred scheme for catalyst regeneration. Nevertheless, it is possible that if the overall plant

capacity is significantly huge, then there will be no significant difference in the MFSPs of both pathways due to economies of scale.

3.3 Sensitivity analysis

Sensitivity analysis explores the effect of ±30% variation in fuel yield, capital cost, operating cost, income tax, discount rate, and electricity generated on the profitability of the two process designs. The sensitivity charts presented in Figs. 7 and 8 depict the effect of changing these parameters on the MSFP of P-2RG and P-1RGC. The grey bar charts show the extent to which the MFSP is sensitive to a 30% increase in a parameter while the blue bar charts depict the sensitivity of the MFSP to a reduction of 30%. The longer the bar chart, the higher the degree of sensitivity of the base MFSP to parameter variations. As it can be seen in Figs. 7 and 8, the MFSPs of both designs have identical sensitivities due to the similarity of the two process schemes and their corresponding costs.

For both designs, a decrease of 30% in fuel yield resulted in a 43% increase in the MFSPs. An increase of 30% in fuel yield, on the other hand, led to a 23% decrease in the MFSPs. This implies that product losses, which can arise from events such as operational and maintenance problems, will have a negative impact on profitability. Conversely, increasing fuel yield will be more economically beneficial for the two process schemes. One way of increasing fuel yield is by increasing plant capacity; however, the associated financial penalty in terms of capital and operating costs has to be weighed accordingly. The MFSP also showed high sensitivity to variations in the operating cost of both designs. An almost linear relationship between the operating cost and the MFSP was observed. An increase of 30% in operating cost resulted in an increase of 27% in the MFSP and *vice versa*. Since a significant proportion of the operating cost is attributed to biomass feed cost as illustrated in Fig. 6, sourcing a less expensive alternative would be a better economic choice. Moreover, heat integration by pinch analysis could hypothetically improve profitability through reductions in utility cost as demonstrated elsewhere [46]. Variations in income tax also influenced profitability to a considerable extent. An increase of 30% in income tax produced an increase of 27% in the MFSP while a 30% reduction in income tax yielded an 18% decrease in the MFSP.

This suggests that income tax reduction or exemptions will be favourable to the profitability of the two process schemes.

The MFSP showed less sensitivity to capital cost, with an increase/decrease of 30% in capital cost producing an increase/decrease of 6% in MFSP. The relatively small effect of an increase in capital cost, along with the substantial influence of an increase in fuel yield on MFSP reinforces that the processes will benefit from economies of scale by increasing plant capacity. Variations in discount rate and electricity generated had minimal influence on the MFSP compared to other parameters.

3.4 Uncertainty analysis

The effect of stochastic variations in fuel yield, capital cost, operating cost, operating income tax, discount rate, and electricity generated on the profitability of the two process schemes was examined by Monte-Carlo simulations to obtain the distributions of the MFSP. Eq. 4 describes the probability density function of the mean MSFP. The likelihood of the MSFP to fall within a particular price interval (a, b) is determined by the area under the curve as shown in Eq. 5.

$$f(x) = \frac{1}{\sqrt{2\pi}\cdot\sigma}\cdot e^{-\frac{1}{2}\cdot\left(\frac{x-\mu}{\sigma}\right)^2} \tag{4}$$

$$P(a \le x \le b) = \int_a^b f(x)\cdot dx \tag{5}$$

The resultant Gaussian distributions of the MFSP of P-2RG and P-1RGC are depicted in Figs. 9 and 10, respectively.

The dashed lines depicted in Figs. 9 and 10 denote the mean values of the MFSP of P-2RG and P-1RGC, respectively. In the case of P-2RG, mean MFSP was observed at £8.72/GGE with a standard deviation of 1.45. For P-1RGC, on the other hand, the mean MFSP value was £8.30/GGE with a standard deviation of 1.39. The unshaded portions of the charts in Figs. 9 and 10 signify 95% probability of the expected MFSPs to be within a specified range. In the case of P-2RG, the expected MFSPs ranged between £5.81/GGE and £11.63/GGE while, for P-1RGC, the expected MFSPs ranged between £5.52/GGE and £11.08/GGE. It is

evident from Figs. 9 and 10 that P-1RGC has a smaller deviation from its mean MFSP compared to P-2PRG.

This implies that 1-PRGC is more economically viable than P-2RG and carries less risk that could result from uncertainty in parameter estimates. Moreover, the observation from the uncertainty analysis is in agreement with the results obtained from the initial economic analysis

4 CONCLUSIONS

The techno-economic assessment of biofuel production from fast pyrolysis of pinewood and subsequent upgrading *via* zeolite cracking has been examined. The model was developed using Aspen Plus®. Two catalyst regeneration configurations (P-2RG and P-1RGC) for bio-oil zeolite upgrading were studied and compared in terms of energy efficiency and profitability.

Although P-1RGC showed a slightly lower energy efficiency of 2% than P-2RG, it exhibited a better economic performance with an MFSP of £7.20/GGE (3.74 % less than P-2RG). The MFSPs of P-1RGC and P-2RG showed similar and significant sensitivities to variations in fuel yield, operating cost and income tax. However, uncertainty analysis further highlighted P-1RGC as the optimal design with a lower mean value of £8.30/GGE and smaller deviation. Sensitivity analysis suggest that increasing plant capacity could make the MFSP more competitive by economies of scale. Overall, income tax reductions, or exemptions will be economically beneficial to biofuel production *via* zeolite upgrading of fast pyrolysis bio-oil regardless of the choice of the regenerator system.

ACKNOWLEDGEMENTS

The authors gratefully acknowledge the financial support for this work by the UK Engineering and Physical Sciences Research Council (EPSRC) project reference: EP/K036548/1 and FP7 Marie Curie iComFluid project reference: 312261.

REFERENCES

[1] IPCC, Summary for Policymakers, In: Climate Change 2014, Mitigation of Climate Change. Contribution of Working Group III to the Fifth Assessment Report of the Intergovernmental Panel on Climate Change, Cambridge University Press, Cambridge,United Kingdom and New York, NY, USA., 2014.

[2] United Nations, Adoption of the Paris Agreement, Paris, France, 2015.

[3] IEA, 2014 Key World Energy Statistics, Paris, France, 2014. http://www.iea.org/publications/freepublications/publication/keyworld2014.pdf.

[4] IEA, Technology roadmap: biofuels for transport, IEA Publications, Paris, France, 2011.

[5] IEA Bioenergy Task 39, The potential and challenges of "drop in" biofuels, 2014. http://task39.org/files/2014/01/Task-39-drop-in-biofuels-report-summary-FINAL-14-July-2014-ecopy.pdf.

[6] A. Locke, G. Henley, A review of the literature on biofuels and food security at a local level, 2014. http://www.odi.org/publications/7801-review-literature-biofuels-food-security-at-local-level (accessed September 9, 2015).

[7] S.N. Naik, V. V Goud, P.K. Rout, A.K. Dalai, Production of first and second generation biofuels: A comprehensive review, Renew. Sustain. Energy Rev. 14 (2010) 578–597. doi:10.1016/j.rser.2009.10.003.

[8] R.H. Sims, W. Mabee, J.N. Saddler, M. Taylor, An overview of second generation biofuel technologies, Bioresour. Technol. 101 (2010) 1570–1580. doi:10.1016/j.biortech.2009.11.046.

[9] S. Czernik, A. V Bridgwater, Overview of Applications of Biomass Fast Pyrolysis Oil, Energy Fuels. 18 (2004) 590–598. doi:10.1021/ef034067u.

[10] S. Xiu, A. Shahbazi, Bio-oil production and upgrading research: A review, Renew. Sustain. Energy Rev. 16 (2012) 4406–4414. doi:http://dx.doi.org/10.1016/j.rser.2012.04.028.

[11] A.K. Hossain, P.A. Davies, Pyrolysis liquids and gases as alternative fuels in internal combustion

406 engines – A review, Renew. Sustain. Energy Rev. 21 (2013) 165–189.
407 doi:10.1016/j.rser.2012.12.031.
408 [12] Y.-H.E. Sheu, R.G. Anthony, E.J. Soltes, Kinetic studies of upgrading pine pyrolytic oil by
409 hydrotreatment, Fuel Process. Technol. 19 (1988) 31–50. doi:http://dx.doi.org/10.1016/0378-
410 3820(88)90084-7.
411 [13] D.C. Elliott, Historical Developments in Hydroprocessing Bio-oils, - Energy Fuels. 21 (2007) 1792–
412 1815. doi:- 10.1021/ef070044u.
413 [14] E. Furimsky, Hydroprocessing challenges in biofuels production, Catal. Today. (2012).
414 doi:10.1016/j.cattod.2012.11.008.
415 [15] P.M. Mortensen, J.-D. Grunwaldt, P.A. Jensen, K.G. Knudsen, A.D. Jensen, A review of catalytic
416 upgrading of bio-oil to engine fuels, Appl. Catal. A Gen. 407 (2011) 1–19.
417 doi:http://dx.doi.org/10.1016/j.apcata.2011.08.046.
418 [16] E. Furimsky, Catalytic hydrodeoxygenation, Appl. Catal. A Gen. 199 (2000) 147–190.
419 doi:http://dx.doi.org/10.1016/S0926-860X(99)00555-4.
420 [17] A.V. Bridgwater, Review of fast pyrolysis of biomass and product upgrading, Biomass and
421 Bioenergy. 38 (2012) 68–94. doi:10.1016/j.biombioe.2011.01.048.
422 [18] J.D. Adjaye, R.K. Sharma, N.N. Bakhshi, Catalytic conversion of wood derived bio-oil to fuels and
423 chemicals, Prog. Catal. 12th Can. Symp. Catal. 73 (1992) 301–308.
424 doi:http://dx.doi.org/10.1016/S0167-2991(08)60828-9.
425 [19] R.K. Sharma, N.N. Bakhshi, Catalytic upgrading of fast pyrolysis oil over hzsm-5, Can. J. Chem.
426 Eng. 71 (1993) 383–391. doi:10.1002/cjce.5450710307.
427 [20] A. de R. Pinho, M.B.B. de Almeida, F.L. Mendes, V.L. Ximenes, L.C. Casavechia, Co-processing
428 raw bio-oil and gasoil in an FCC Unit, Fuel Process. Technol. 131 (2015) 159–166.
429 doi:10.1016/j.fuproc.2014.11.008.
430 [21] J.D. Adjaye, S.P.R. Katikaneni, N.N. Bakhshi, Catalytic conversion of a biofuel to hydrocarbons:

effect of mixtures of HZSM-5 and silica-alumina catalysts on product distribution, Fuel Process. Technol. 48 (1996) 115–143. doi:http://dx.doi.org/10.1016/S0378-3820(96)01031-4.

[22] H. Zhang, R. Xiao, H. Huang, G. Xiao, Comparison of non-catalytic and catalytic fast pyrolysis of corncob in a fluidized bed reactor, Bioresour. Technol. 100 (2009) 1428–1434. doi:http://dx.doi.org/10.1016/j.biortech.2008.08.031.

[23] T.R. Carlson, Y.-T. Cheng, J. Jae, G.W. Huber, Production of green aromatics and olefins by catalytic fast pyrolysis of wood sawdust, Energy Environ. Sci. 4 (2010) 145–161. doi:-10.1039/C0EE00341G.

[24] A. Dutta, A. Sahir, E. Tan, D. Humbird, L.J. Snowden-Swan, P. Meyer, J. Ross, D. Sexton, R. Yap, J.L. Lukas, Process Design and Economics for the Conversion of Lignocellulosic Biomass to Hydrocarbon Fuels. Thermochemical Research Pathways with In Situ and Ex Situ Upgrading of Fast Pyrolysis Vapors, (2015) 275. doi:10.2172/1215007.

[25] Y.S. Choi, K.-H. Lee, J. Zhang, R.C. Brown, B.H. Shanks, Manipulation of chemical species in bio-oil using in situ catalytic fast pyrolysis in both a bench-scale fluidized bed pyrolyzer and micropyrolyzer, Biomass and Bioenergy. 81 (2015) 256–264. doi:http://dx.doi.org/10.1016/j.biombioe.2015.07.017.

[26] G. Liu, M.M. Wright, Q. Zhao, R.C. Brown, Catalytic fast pyrolysis of duckweed: Effects of pyrolysis parameters and optimization of aromatic production, J. Anal. Appl. Pyrolysis. 112 (2015) 29–36. doi:http://dx.doi.org/10.1016/j.jaap.2015.02.026.

[27] P.T. Williams, N. Nugranad, Comparison of products from the pyrolysis and catalytic pyrolysis of rice husks, Energy. 25 (2000) 493–513. doi:http://dx.doi.org/10.1016/S0360-5442(00)00009-8.

[28] M.A. Jackson, D.L. Compton, A.A. Boateng, Screening heterogeneous catalysts for the pyrolysis of lignin, Pyrolysis 2008 Pap. Present. 18th Int. Symp. Anal. Appl. Pyrolysis. 85 (2009) 226–230. doi:http://dx.doi.org/10.1016/j.jaap.2008.09.016.

[29] A. Pattiya, J.O. Titiloye, A. V Bridgwater, Fast pyrolysis of cassava rhizome in the presence of

456 catalysts, J. Anal. Appl. Pyrolysis. 81 (2008) 72–79.
457 doi:http://dx.doi.org/10.1016/j.jaap.2007.09.002.
458 [30] J. Adam, M. Blazsó, E. Mészáros, M. Stöcker, M.H. Nilsen, A. Bouzga, J.E. Hustad, M. Grønli, G.
459 Øye, Pyrolysis of biomass in the presence of Al-MCM-41 type catalysts, Fuel. 84 (2005) 1494–
460 1502. doi:http://dx.doi.org/10.1016/j.fuel.2005.02.006.
461 [31] Q. Lu, Z. Zhang, C. Dong, X.-F. Zhu, Catalytic Upgrading of Biomass Fast Pyrolysis Vapors with
462 Nano Metal Oxides , Energies. 3 (2010) 1805–1820.
463 [32] J.D. Adjaye, N.N. Bakhshi, Production of hydrocarbons by catalytic upgrading of a fast pyrolysis
464 bio-oil. Part II: Comparative catalyst performance and reaction pathways, Fuel Process. Technol. 45
465 (1995) 185–202. doi:10.1016/0378-3820(95)00040-E.
466 [33] S. Tan, Z. Zhang, S. Jianping, Q. Wang, Recent progress of catalytic pyrolysis of biomass by
467 HZSM-5, Chinese J. Catal. 34 (2013) 641–650. doi:10.1016/S1872-2067(12)60531-2.
468 [34] M.S. Talmadge, R.M. Baldwin, M.J. Biddy, R.L. McCormick, G.T. Beckham, G. a Ferguson, S.
469 Czernik, K. a Magrini-Bair, T.D. Foust, P.D. Metelski, C. Hetrick, M.R. Nimlos, A perspective on
470 oxygenated species in the refinery integration of pyrolysis oil, Green Chem. 16 (2014) 407.
471 doi:10.1039/c3gc41951g.
472 [35] Hydrocarbon Publishing, Fluid Catalytic Cracking (FCC) - Future Roles of FCC and
473 Hydroprocessing Units in Modern Refineries, (n.d.).
474 http://www.hydrocarbonpublishing.com/ReportP/fcc.php (accessed December 2, 2015).
475 [36] J. Gary, G. Handwerk, Petroleum Refining Technology and Economics, Marcel Dekker Inc, New
476 York, 1984.
477 [37] R. Thilakaratne, T. Brown, Y. Li, G. Hu, R. Brown, Mild catalytic pyrolysis of biomass for
478 production of transportation fuels: a techno-economic analysis, Green Chem. 16 (2014) 627–636.
479 doi:10.1039/C3GC41314D.
480 [38] B. Li, L. Ou, Q. Dang, P. Meyer, S. Jones, R. Brown, M. Wright, Techno-economic and uncertainty

analysis of in situ and ex situ fast pyrolysis for biofuel production., Bioresour. Technol. 196 (2015) 49–56. doi:10.1016/j.biortech.2015.07.073.

[39] Y. Zhang, T.R. Brown, G. Hu, R.C. Brown, Techno-economic analysis of two bio-oil upgrading pathways, Chem. Eng. J. (2013). doi:10.1016/j.cej.2013.01.030.

[40] M. Shemfe, S. Gu, P. Ranganathan, Techno-economic performance analysis of biofuel production and miniature electric power generation from biomass fast pyrolysis and bio-oil upgrading, Fuel. 143 (2015) 361–372. doi:http://dx.doi.org/10.1016/j.fuel.2014.11.078.

[41] E. Ranzi, T. Faravelli, A. Frassoldati, G. Migliavacca, S. Pierucci, S. S., Chemical Kinetics of Biomass Pyrolysis, - Energy Fuels. (2008) 4292. doi:- 10.1021/ef800551t.

[42] X. Wang, S.R.A. Kresten, W. Prins, P.M.W. Van Swaaij, Biomass Pyrolysis in a Fluidized Bed Reactor. Part 2: Experimental Validation of Model Results, - Ind. Eng. Chem. Res. (2005) 8786-8795. doi:- 10.1021/ie050486y.

[43] M.M. Wright, D.E. Daugaard, J.A. Satrio, R.C. Brown, Techno-economic analysis of biomass fast pyrolysis to transportation fuels, 2010. doi:10.1016/j.fuel.2010.07.029.

[44] M. Glantz, Scientific financial management advances in intelligence capabilities for corporate valuation and risk assessment, AMACOM, New York, 2000.

[45] L. Ou, R. Thilakaratne, R.C. Brown, M.M. Wright, Techno-economic analysis of transportation fuels from defatted microalgae via hydrothermal liquefaction and hydroprocessing, Biomass and Bioenergy. 72 (2015) 45–54. doi:10.1016/j.biombioe.2014.11.018.

[46] M.B. Shemfe, B. Fidalgo, S. Gu, Heat integration for bio-oil hydroprocessing coupled with aqueous phase steam reforming, Chem. Eng. Res. Des. (2015). doi:10.1016/j.cherd.2015.09.004.

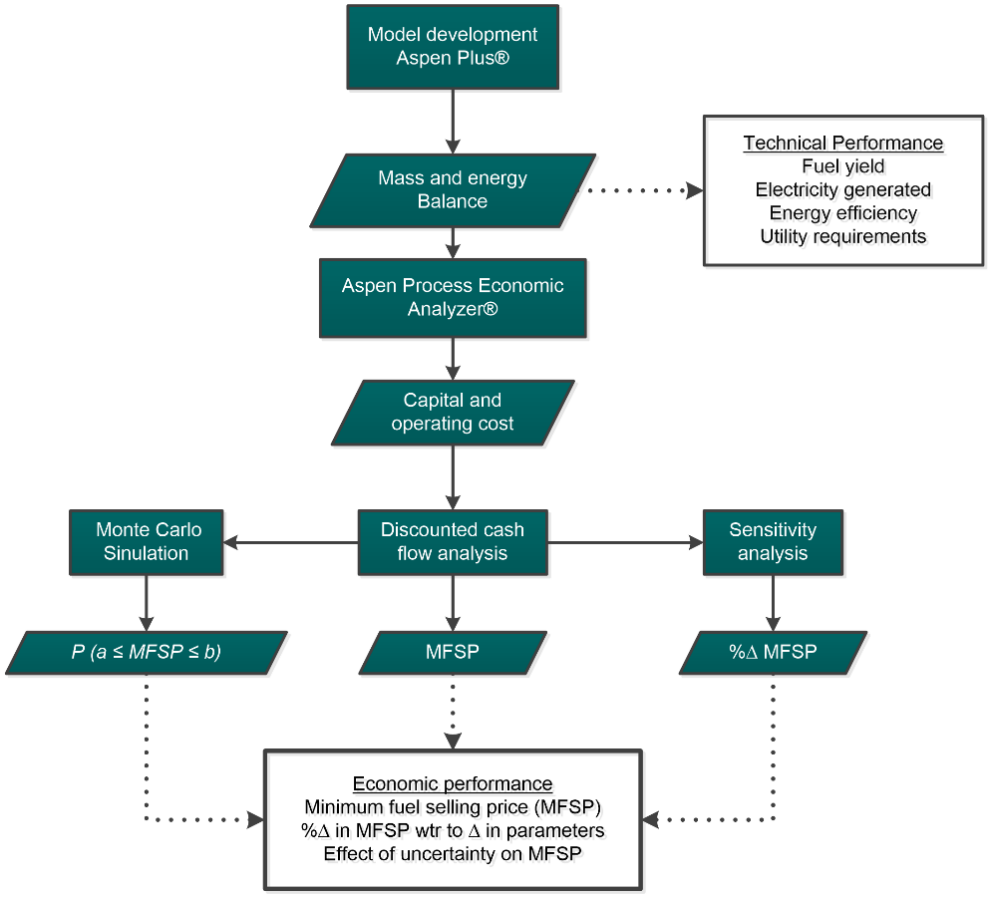
Model development
Aspen Plus®
Mass and energy
Balance
Technical Performance
Fuel yield
Electricity generated
Energy efficiency
Utility requirements
Aspen Process Economic
Analyzer®
Capital and
operating cost
Monte Carlo
Sinulation
Discounted cash
flow analysis
Sensitivity
analysis
P (a ≤ MFSP ≤ b)
MFSP
%Δ MFSP
Economic performance
Minimum fuel selling price (MFSP)
%Δ in MFSP wtr to Δ in parameters
Effect of uncertainty on MFSP

Fig. 1

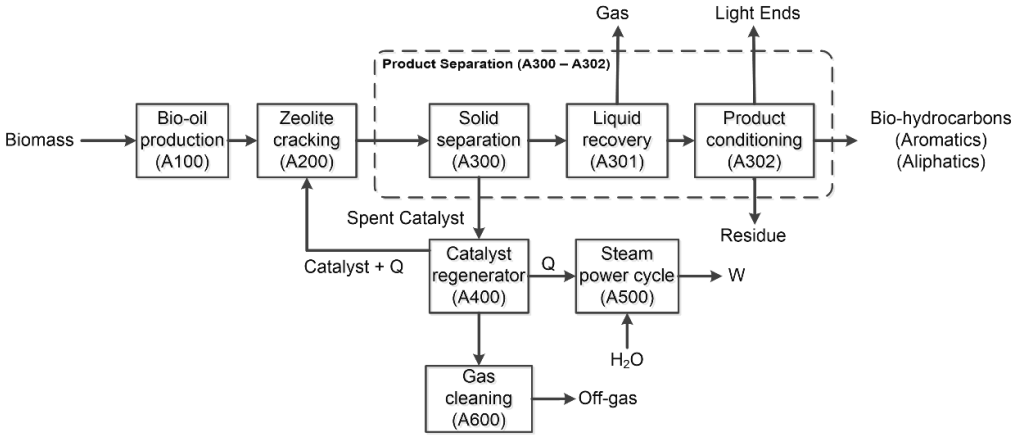
Gas
Light Ends
Product Separation (A300 – A302)
Biomass
Bio-oil production (A100)
Zeolite cracking (A200)
Solid separation (A300)
Liquid recovery (A301)
Product conditioning (A302)
Bio-hydrocarbons (Aromatics) (Aliphatics)
Spent Catalyst
Residue
Catalyst + Q
Catalyst regenerator (A400)
Q
Steam power cycle (A500)
W
H2O
Gas cleaning (A600)
Off-gas

Fig. 2.

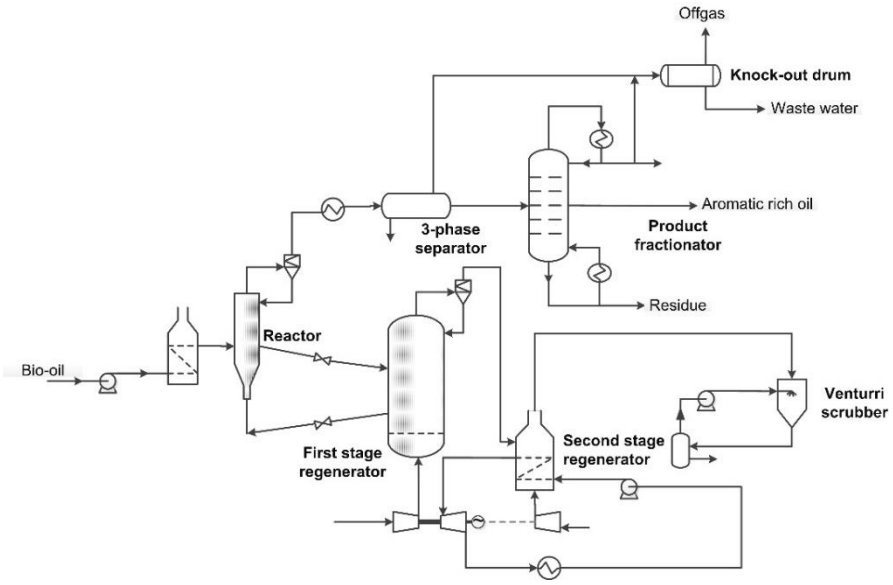
Offgas
Knock-out drum
Waste water
Aromatic rich oil
3-phase separator
Product fractionator
Residue
Reactor
Bio-oil
Venturri scrubber
First stage regenerator
Second stage regenerator

Fig. 3

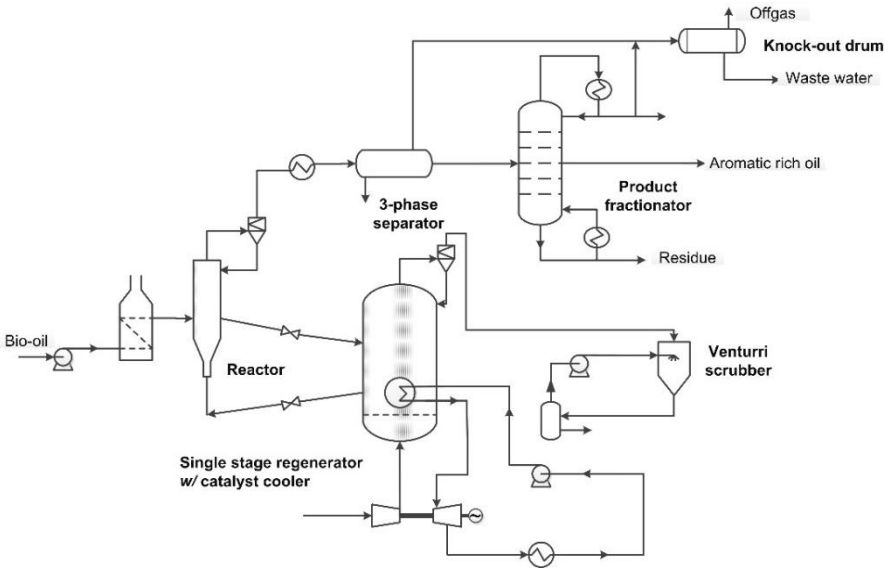
Offgas
Knock-out drum
Waste water
Aromatic rich oil
Product fractionator
3-phase separator
Residue
Bio-oil
Reactor
Venturri scrubber
Single stage regenerator w/ catalyst cooler

Fig. 4.

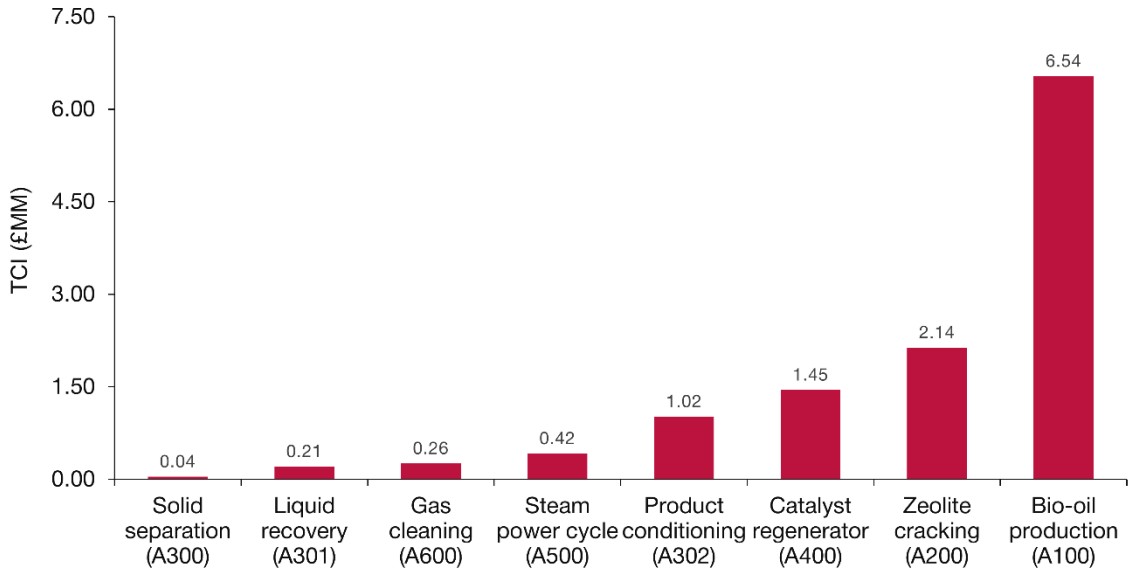
7.50
6.00
4.50
3.00
1.50
0.00
TCI (£MM)
0.04
0.21
0.26
0.42
1.02
1.45
2.14
6.54
Solid separation (A300)
Liquid recovery (A301)
Gas cleaning (A600)
Steam power cycle (A500)
Product conditioning (A302)
Catalyst regenerator (A400)
Zeolite cracking (A200)
Bio-oil production (A100)

Fig. 5a.

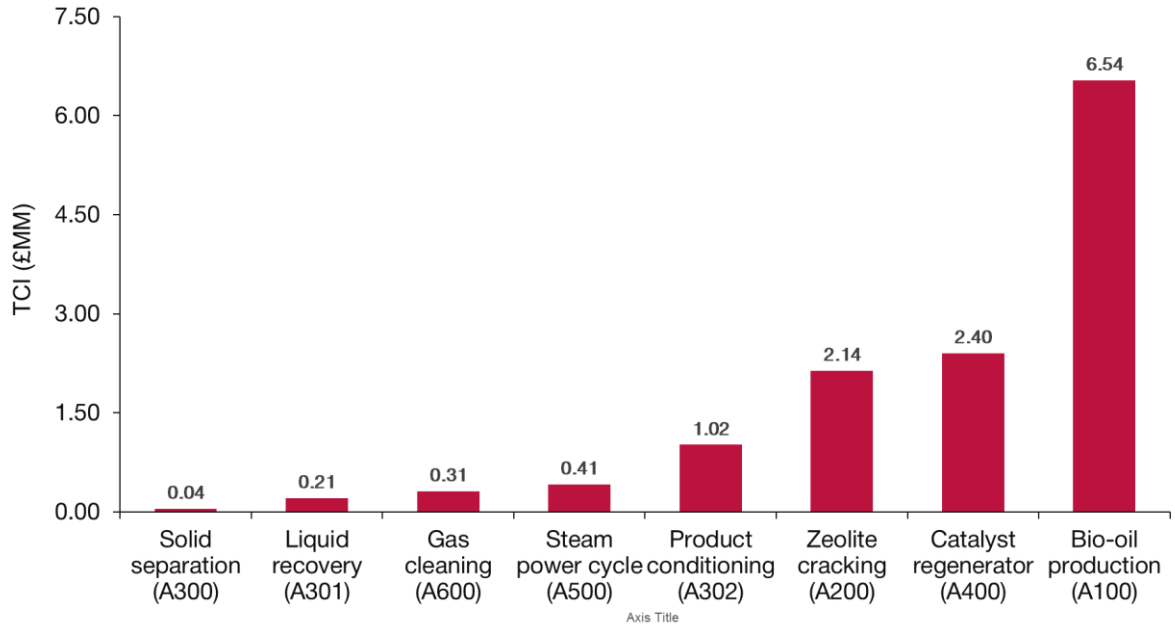
7.50
6.00
4.50
3.00
1.50
0.00
TCI (£MM)
0.04
0.21
0.31
0.41
1.02
2.14
2.40
6.54
Solid separation (A300)
Liquid recovery (A301)
Gas cleaning (A600)
Steam power cycle (A500)
Product conditioning (A302)
Zeolite cracking (A200)
Catalyst regenerator (A400)
Bio-oil production (A100)
Axis Title

Fig. 6b.

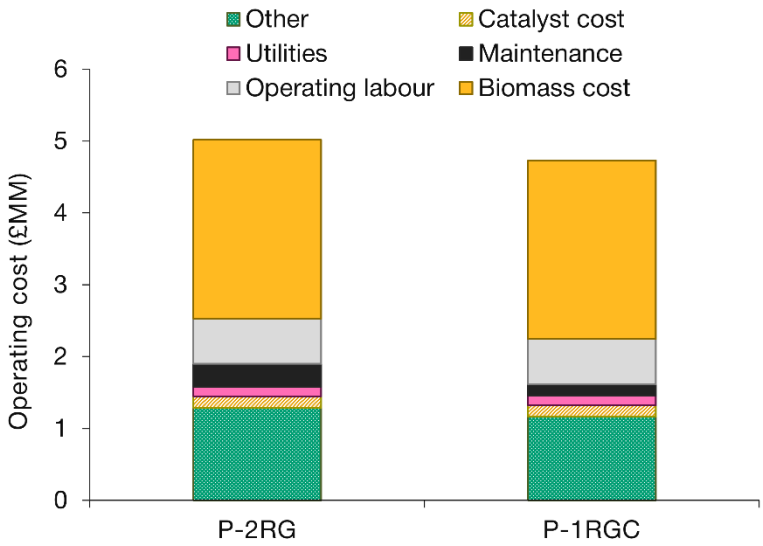
Other
Catalyst cost
Utilities
Maintenance
Operating labour
Biomass cost
Operating cost (£MM)
0
1
2
3
4
5
6
P-2RG
P-1RGC

Fig. 7.

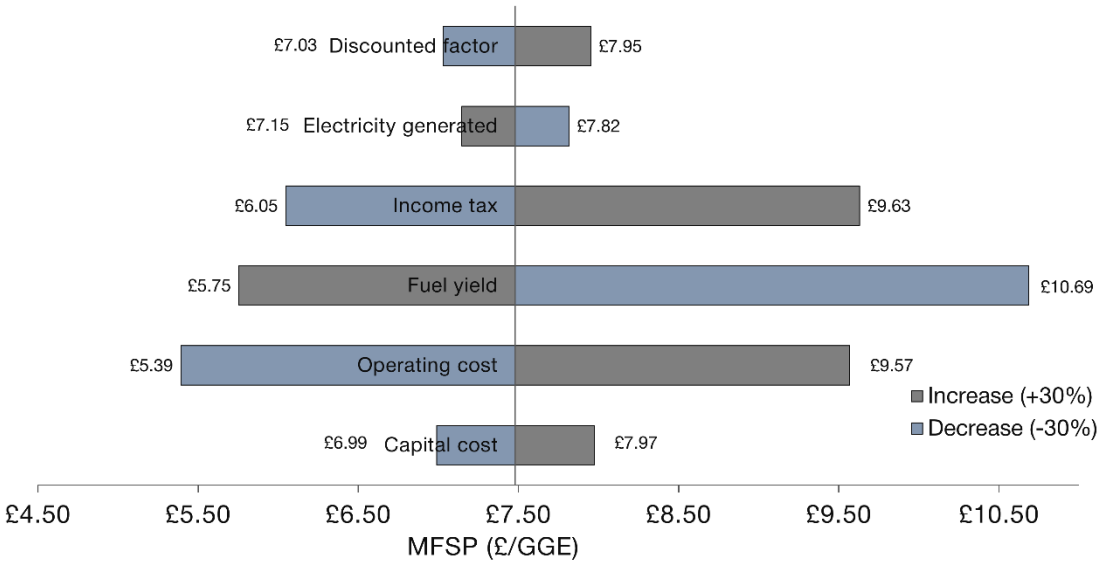
£7.03
Discounted factor
£7.95
£7.15
Electricity generated
£7.82
£6.05
Income tax
£9.63
£5.75
Fuel yield
£10.69
£5.39
Operating cost
£9.57
£6.99
Capital cost
£7.97
Increase (+30%)
Decrease (-30%)
£4.50
£5.50
£6.50
£7.50
£8.50
£9.50
£10.50
MFSP (£/GGE)

Fig. 8.

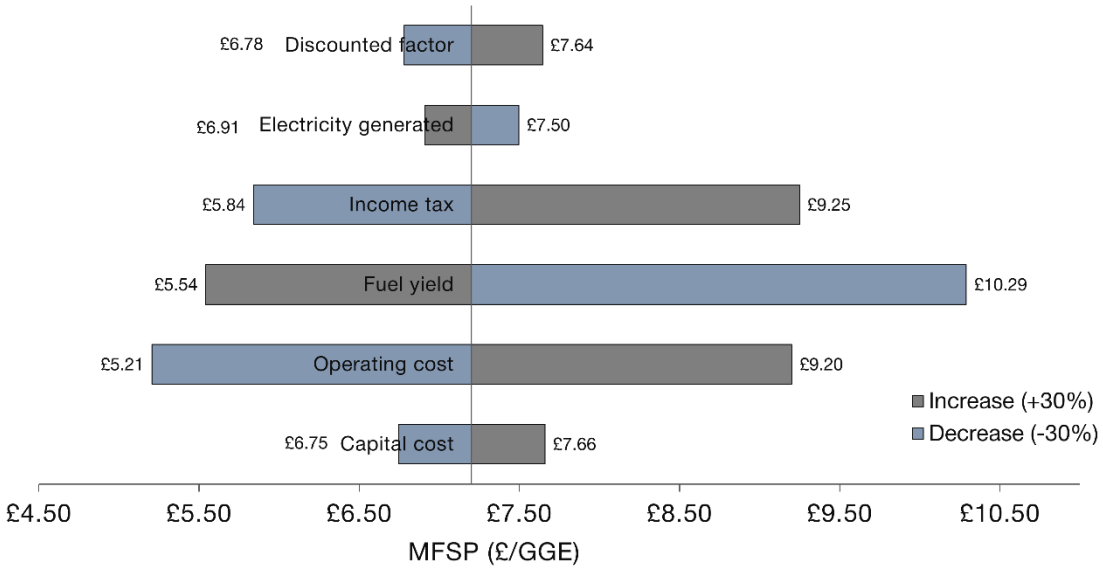
£6.78
Discounted factor
£7.64
£6.91
Electricity generated
£7.50
£5.84
Income tax
£9.25
£5.54
Fuel yield
£10.29
£5.21
Operating cost
£9.20
£6.75
Capital cost
£7.66
Increase (+30%)
Decrease (-30%)
£4.50
£5.50
£6.50
£7.50
£8.50
£9.50
£10.50
MFSP (£/GGE)

Fig. 9.

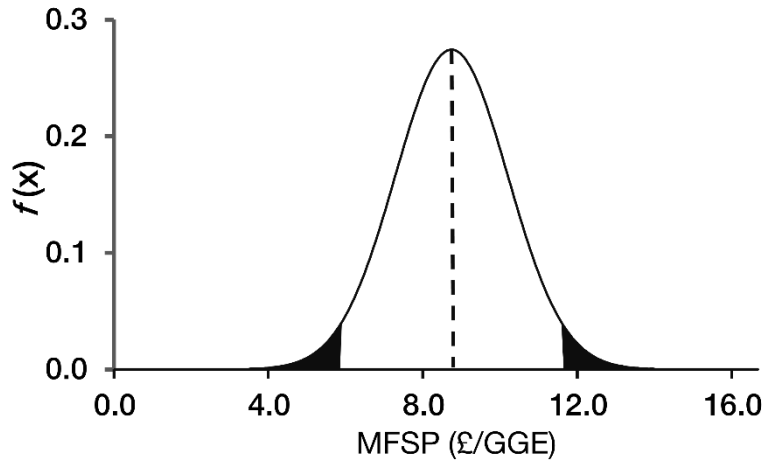

Fig. 10

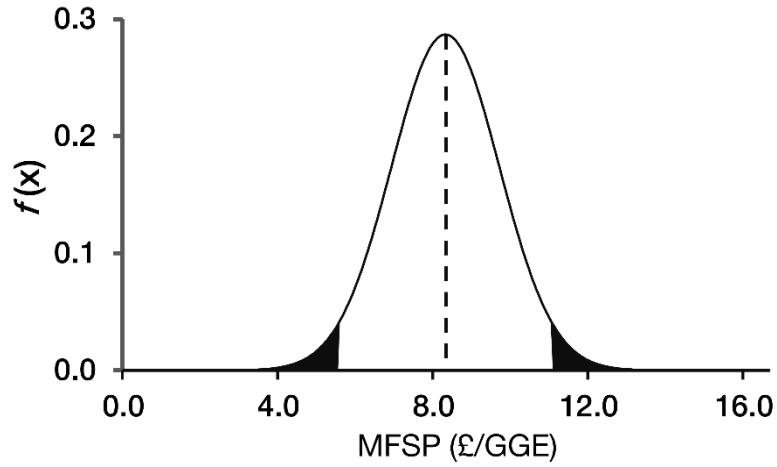

Fig. 11

Table 1 Composition of bio-oil feedstock [40, 46]

Component	**(wt.%)**
Alcohols	
Methanol	2.69
Ethanol	1.24
Aldehyde & Ketones	
Formaldehyde	3.43
Glyoxal	0.64
Acetone	1.08
Hydroxymethylfurfural	1.82
Hydroxyacetaldehyde	3.30
Acids	
Acrylic	0.01
Acetic acid	0.14
Phenolics	
Phenol	0.74
*p*Coumaryl	1.48
Lignin derivatives	12.47
Lumped phenolics	1.37
Sugars	
Levoglucosan	48.39
Xylan	0.36
Water	20.61

Table 2 Product distribution of zeolite cracking at 370 °C and WHSV of 3.6hr^{-1} [18]

Component	wt.%
Organics	*38.7*
Aliphatics hydrocarbons	0.50
Aromatics hydrocarbons	26.66
Phenols	3.75
Acids	0.39
Ethers	0.31
Ketones	0.19
Alcohols	0.31
Unidentified	6.58
Gas	*9.20*
Residue	*0.50*
Water	*28.10*
*Char**	*10.2*
*Coke**	*9.8*
*Unaccounted***	*3.5*

**Assumed coke= char + coke*
***Unaccounted assumed as residue*

Table 3 Product distribution of product

Components	**wt. %**
Aliphatic hydrocarbons	1.75
Aromatic hydrocarbons	94.72
Phenols	0.01
Acids	0.27
Ethers	0.16
Ketones	0.61
Alcohols	0.88
*Carbon Residue**	1.60

**Unidentified components assumed as carbon residue*

Table 4 Operating cost parameters

Material	**Cost**
Biomass cost [£/t][39]	90
HZSM-5 catalyst [£/kg]	198
Ash disposal [£/t]	0.11
Utilities	
Electricity [£/kWh][39]	0.15
Cooling water [£/m^3]	0.032
Natural Gas [£/kWh][39]	0.049

Table 5 Inputs for DCF analysis.

Economic Inputs	
Required Rate of Return (r)	10%
Plant lifetime (t)	20 years
Capital Cost Escalation	5%
Revenue Escalation	5%
Operating Cost Escalation	3%
Income Tax	40%

Table 6 Parameters and range of variation for uncertainty analysis

Parameter	Range of variation
Fuel yield (GGE/yr)	±30%
Capital cost (£)	-20% to +50%
Operating cost (£)	-10% to +30%
Income tax (%)	±25%
Discount rate (%)	±30%
Electricity generated (kW)	±30%

Table 7 Mass and Energy Balance per hour basis

Process inputs		
Fast Pyrolysis		
Biomass (kg/h)	3,000	
Zeolite Cracking	**P-2RG**	**P-1RGC**
Bio-oil(kg/h)	1,608	1,608
Electricity (kWh)	123	138
Fired Heater (pre-heater)	55	55
Process Outputs		
Fuel yield (kg/h)	448	448
Net electricity (kWh)	896	747
Energy Efficiency (%)	54	52